16TH EUROPEAN CONFERENCE ON
EARTHQUAKE ENGINEERING
THESSALONIKI
18 - 21 JUNE 2018

AFTERSHOCK FORECASTING EXPERIMENT FOR BUSHEHR PROVINCE OF IRAN USING THE EPIDEMIC-TYPE AFTERSHOCK SEQUENCE (ETAS) MODEL

Hamid Reza TAVAKOLI[1], Nader DAVOODI[2], Abdollah JALILIAN[3], Mehdi ZARE[4]

ABSTRACT

Forecasting aftershock probabilities or forecasting the expected number of aftershocks, immediately after occurrence of an earthquake with a specified magnitude, is very important in risk management. The Epidemic-Type Aftershock Sequence (ETAS) model is a prominent stochastic model which describes the occurrence of earthquake sequences. However, this model has never been used to forecast aftershocks in Iran.
Bushehr province in southern Iran has a long coastline onto the Persian Gulf and is one of the most strategic regions in the Middle East due to its major petroleum exporting ports, the industrial corridors and of course Bushehr Nuclear Power Plant. Bushehr is located in Zagros seismic region of Iran plateau. The earthquakes in this region often have a shallow focal depth and a reverse faulting mechanism. In this study, we simulate and estimate the number of aftershocks of the Mw 6.3 earthquake that took place in this region on April 9,2013, using the ETAS model. An earthquake catalog has been extracted from areas around Bushehr. By fitting ETAS model on this catalog, we conducted a short-term earthquake forecasting experiment for Bushehr province in Iran. The results were satisfactory and the Epidemic-Type Aftershock Sequence (ETAS) model proved as a reliable model in forecasting aftershocks probabilities and subsequently aftershock advisory.

Keywords: Aftershocks probabilities; Earthquake forecasting; Bushehr province of Iran; ETAS model

1. INTRODUCTION

Typically, many aftershocks will occur after a large earthquake in the area surrounding the mainshock location. Aftershocks will occur during a time span (days to years) following the mainshock. The average rate of aftershocks is dependent on mainshock magnitude, Mm. this rate decreases with an increase in elapsed time from the mainshock occurrence (Yeo et al. 2005).
Forecasting aftershock probabilities, as already as possible after a mainshock, is required to mitigate the risks in disaster area (Omi et al. 2014). Aftershock may cause collapse of buildings that already damaged (but not yet repaired) by the mainshock. There are many examples that the buildings residents evacuate the buildings after the mainshock due to fearing of collapse of the damaged buildings in aftershocks (Yeo et al. 2005). There has not been proposed a method to predict the occurrence of earthquakes (mainshock or aftershock). However, some effective statistical approaches have been developed to forecast aftershock probabilities (Luen 2010). Among the developed methods to describe earthquake sequences, the epidemic-type aftershock sequence (ETAS) model is the most widely used model by researchers. The ability of this statistical approach in aftershock sequences modeling is widely accepted from the scientific community. (See Ogata 1998,1999,2006 and 2011; Console et al. 2010; Lombardi and Marzocchi 2010; Zhuang 2002, 2011, 2012; Stiphout et al. 2012). Despite the importance of aftershocks in the earthquake risk management, so far, few studies have

[1]Associate Professor, Civil Engineering, Noshirvani University of Technology, Babol, Iran, tavakoli@nit.ac.ir
[2]Phd Student, Civil Engineering, Noshirvani University of Technology, Babol, Iran, naderdawoodi@gmail.com
[3]Assistant Professor, Department of Statistics ,Razi University, Kermanshah, Iran, jalilian @ razi.ac.ir
[4]Professor, International Institute of Earthquake Engineering and Seismology, Tehran, Iran, mzare@ iiees.ac.ir

been conducted in this regard in Iran. Omi et al. (2016) investigate the Iranian earthquake catalog to select 15 earthquakes between 2002 to 2013 and studied their sequence parameters by calculating modified Omori law parameters. they used three declustering methods: 1) the Gardner and Knopoff method (1974); 2) a modified version spatial windowing based on the Wells and Copersmith relation (1994); and 3), the Burkhard and Gruenthal method(2009) to collect the aftershocks catalog.

In this study, we try to forecast aftershocks occurrence following April 9, 2013, Kaki region earthquake (with moment magnitude of Mw = 6.3) in Bushehr province in Iran. To this end, in the first step, we provide the earthquake catalog of Bushehr province surrounding areas in south of Iranian plateau from data center of International Institute of Earthquake Engineering and Seismology (available at: http://www.iiees.ac.ir/fa/eqcatalog/). This catalog is consist of 454 earthquakes that occurred at rectangular geographical region (bounded in 27.5°-31° N and 50°-53° E) from 1/1/1983 to 8/4/2013. To prepare a unified catalog ,all existing magnitude scales in the provided catalog are converted to the moment magnitude scale, using conversation relations provided by shahvar et al (shahvar et al. 2013). moment magnitude is the most appropriate magnitude scale in seismology which is not saturated for large earthquakes and has a physical meaning (Kanamori 1977). The magnitude threshold Mw = 4.0 and the start date of 1/1/1983 is chosen according to Zare et.al (2014) and by considering the Iran seismic network development. In the next step, an ETAS model is used to calculate the aftershock parameters. Finally, using ETAS parameters, we forecast aftershocks occurrence following Bushehr earthquake in April 9, 2013

2.THE 2013 KAKI EARTHQUAKE

In April 9, 2013at 11:52 UTC (16:22 local time), an Mw 6.3 earthquake struck the Kaki and Borazjan region in Southof Iran(bushehr province). It has been reported that this earthquake had 37 victims and more than 950 injured people. Up to 10 a.m. in the next day, nearly 100 aftershocks were recorded and reported by Iranian Seismological Center (http://irsc.ut.ac.ir/). By April 23, about 145 aftershocks with magnitude between 2.8 to 5.4 occurred in the area around kaki. In the first 20 hours after the mainshock, 62 aftershocks with a magnitude greater than 3.6 occurred in the epicentral region, mostly in the east and north of the epicenter. The largest aftershock with magnitude ml=5.3 occurred 14 hours after the mainshock. The shock was strongly felt in Kaki (assessed VII, 18 km southwest of epicenter). Also, according to reports, no damages were observed in nuclear power plant of Bushehr (80 Km NW of the epicenter). (zare and shahvar. 2013). A map of aftershocks up to two weeks after kaki earthquake is shown in Figure.1.

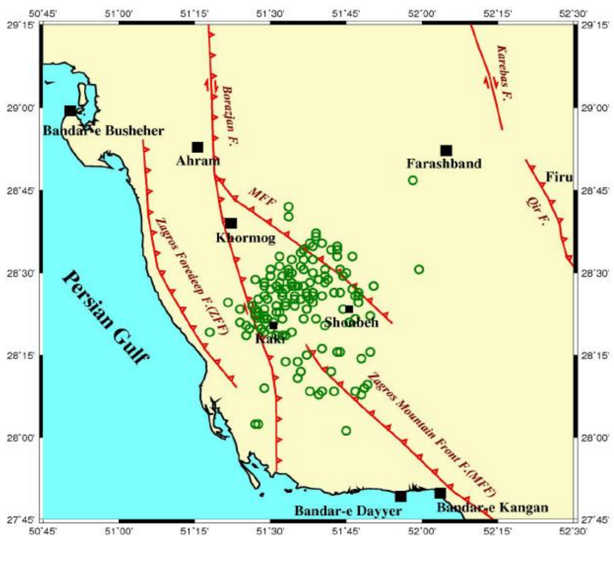

Figure 1. Map of aftershocks up to two weeks after kaki earthquake (Eslami et al. 2013 kaki earthquake report, http://www.iiees.ac.ir)

According to the EMSC (European-Mediterranean Seismological Centre), the earthquake exhibited nearlya pure focal mechanism with NW–SE fault plane, with a focal depth of 10 km. Other reports on Focal mechanisms (i.e. by USGS) showed mostly compressional having a strike-slip component. The most important fault in the epicentral region is in the Borazjan fault, having a north-south strike with a NNW-SSE trend. The fault segment is about 100km which is located in the east of the Mond Anticline, ranged from the western parts of the Jashk Salt-Diapir (locally known as Kuh-e Namak) (zare and shahvar. 2013). The intensity and PGA Shake Maps generated by IIEES are shown in Figure.2 based on magnitude and epicenter.

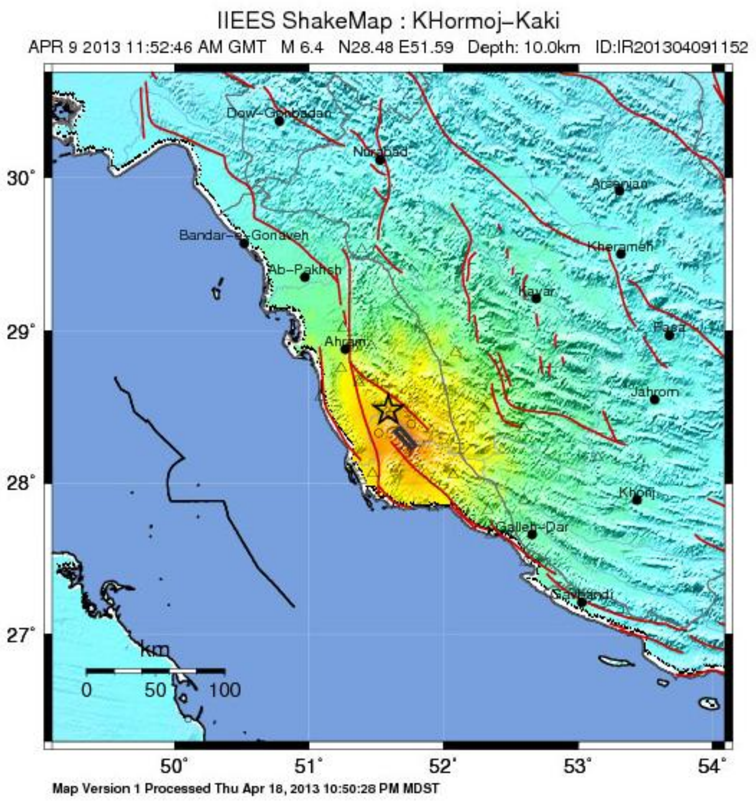

PERCEIVED SHAKING	Not felt	Weak	Light	Moderate	Strong	Very strong	Severe	Violent	Extreme
POTENTIAL DAMAGE	none	none	none	Very light	Light	Moderate	Moderate/Heavy	Heavy	Very Heavy
PEAK ACC.(%g)	<0.17	0.17–1.4	1.4–4.0	4.0–9	9–17	17–32	32–61	61–114	>114
PEAK VEL.(cm/s)	<0.12	0.12–1.1	1.1–3.4	3.4–8	8–16	16–31	31–59	59–115	>115
INSTRUMENTAL INTENSITY	I	II–III	IV	V	VI	VII	VIII	IX	X+

Scale based upon Shahvar, et al.; 2013

Figure 2. Shake Map of the event generated by the IIEES (http://www.iiees.ac.ir)

3. ETAS MODEL

In general, an earthquake catalog is consisting of the time (t), longitude(x) and latitude(y) of epicenter and magnitude (m) of earthquakes. Thus any catalog with N earthquake can be represented by a point pattern (t_i, x_i, y_i, m_i): $i = 1, \dots, N$. This space-time point-process model can be described by the epidemic type aftershock sequence (ETAS) model. In ETAS model each earthquake has a computable probability to be a background (spontaneous) event or triggered by a previous event (Ogata 1998). The basis of this model is to find a mathematical function that can describe the seismic branching sequences in a given area. Roughly, this branching point processes can be defined by the conditional intensity function as equation 1(Ogata 1998):

$$\lambda(t, x, y|\mathcal{H}_t) = \mu(x, y) + \sum_{\{i:t_i<t\}} \kappa(mi)\, g(t - ti)\, f(x - xi, y - yi; mi) \quad (1)$$

Where $\mathcal{H}_t = \{ (t_i, x_i, y_i, m_i); t_i < t \}$ is the history of the earthquakes occurrence up to time t (Ogata 1998; Zhuang et al. 2002). μ(x, y) (unit: events/(day·deg2)) is the background seismicity rate, which is a function of spatial locations but constant over time, and $\kappa(m_i)\, g(t - t_i)\, f(x - x_i, y - y_i; m_i)$ (unit: events/(day·deg2))(is described in Equations 2, 3, and 4 .) is the contribution to seismicity rate by the event i that has already occurred (Zhuang 2011).

$$k_{A,\alpha}(m_i) = A \exp[\alpha(m_i - m_0)] \tag{2}$$

(Unit: events) is the expected number of aftershocks produced by an earthquake of magnitude m_i based on the Gutenberg-Richter law . A > 0 and $\alpha > 0$ are unknown parameters.

$$g_{c,p}(t - t_i) = \begin{cases} \frac{(P-1)}{C}\left(1 + \frac{t-t_i}{C}\right)^{-P} & t - t_i > 0 \\ 0 & t - t_i \leq 0 \end{cases} \tag{3}$$

(Unit: day−1) is the probability density function of the length of the time interval between an earthquake and its aftershocks which is defined based on the modified Omori's law. c > 0 and p > 1 are unknown parameters.

$$f_{D,\gamma,q}(x - x_i, y - y_i | m_i) = \frac{q-1}{\pi D \exp[\gamma(m_i - m_0)]}\left(1 + \frac{(x-x_i)^2 + (y-y_i)^2}{D \exp[\gamma(m_i - m_0)]}\right)^{-q} \tag{4}$$

(Unit: deg−2) is the probability density function of the relative locations between the earthquake and its aftershocks (Zhuang 2011). D > 0, $\gamma > 0$ and q > 1 are unknown parameters.
The unknown model parameters $\theta(\mu, A, \alpha, c, p, D, \gamma, q)$ are estimated by fitting the ETAS model on the earthquake catalog using an iterative approach (maximizing the log-likelihood function) proposed by Zhuang et al. (2002).

Given the history of the earthquakes occurrence up to time t, to forecast occurring of earthquakes in the next time interval $[t, t + \Delta t]$ in a region S, equation 5 can be used directly(Zhuang 2011) (also see Helmstetter et al. (2006)):

$$\Lambda([t, t + \Delta t] \times S) = \iint_S \int_t^{t+\Delta t} \lambda(t, x, y)\, dt\, dx\, dy \tag{5}$$

Where $\Lambda([t, t + \Delta t] \times S)$ is the expected number of earthquakes occurring in [t, t + t] × S . Consequently, the probability of occurring at least one event is (Zhuang 2011):

$$P\{N([t, t + \Delta t] \times S) \geq 0\} = 1 - \exp\left\{- \iint_S \int_t^{t+\Delta t} \lambda(t, x, y)\, dt\, dx\, dy\right\} \tag{6}$$

In this study, the R (R Core Team 2016) package of ETAS from the Comprehensive R Archive Network (CRAN) available at http://CRAN.R-project.org/package=ETAS and GitHub at https://github.com/jalilian/ETAS has been used (under GPL 2 license).

4. APPLICATION OF ETAS MODEL, DISCUSSION AND RESULTS

Some of R package ETAS software outputs are shown in Figures 3, 4 and 5. Figure 3 shows the spatial distribution of earthquakes occurring at rectangular region (bounded in 27.5°-31° N and 50°-53° E) from 1/1/1983 to 8/4/2013. In figure 4 the plot of log10(Nm) versus m (Gutenberg-Richter law), the plot of log10(Nt) versus t and the distribution of earthquake magnitude versus the time t is shown. Where m is the magnitude of earthquakes, Nm is the number of each magnitude in catalog and Nt is the number of earthquakes that occurred up to time t.

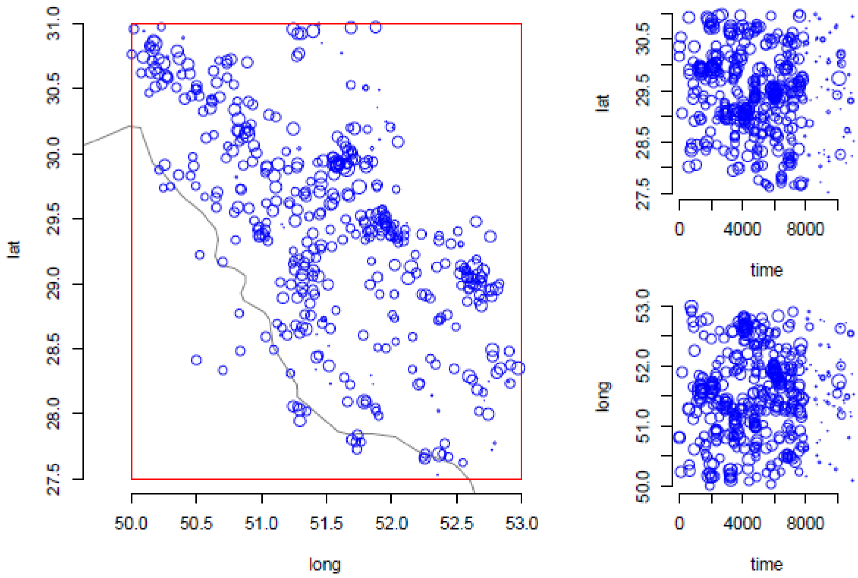

Figure 3. Plot of earthquake catalog in time interval 1/1/1983 to 8/4/2013. Circle with a larger radius, indicating earthquakes with greater magnitudes.

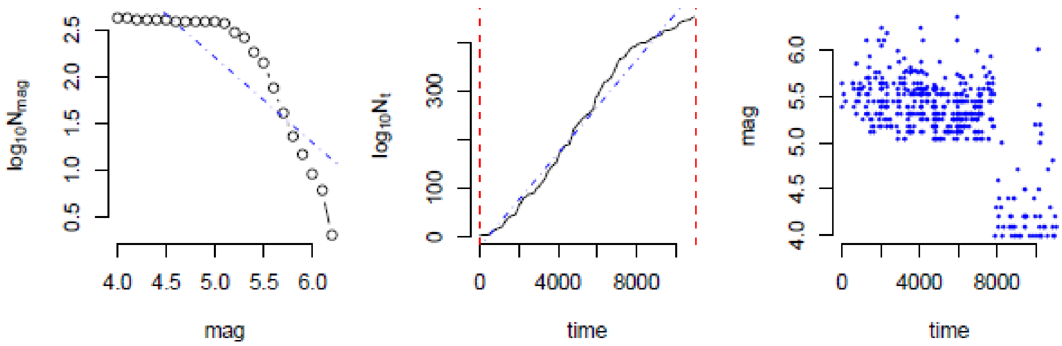

Figure 4. Left : Plot of Gutenberg-Richter law , middle : number of earthquakes versus the time, Right : distribution of earthquake magnitudes in the time interval 1/1/1983 to 8/4/2013.

The model parameters $\theta(\mu, A, \alpha, c, p, D, \gamma, q)$ in equations 2, 3 and 4, are estimated by fitting the ETAS model on the earthquake catalog. The final parameters of ETAS model for Bushehr region are presented in table 1. The plot of background seismicity rate and clustering coefficient are shown in figure 5. Clustering coefficient is the ratio of the spatial clustering intensity (in right hand side of equation 1) to the total intensity (See Zhuang 2002). It can be seen from figure 5 that the clustering coefficient in most part of study area is between 0.4 to 0.8 and some points have higher values.

Table 1. Final ETAS model parameters for Bushehr region.

Parameter	**Value**
μ	1.040906e+00
A	3.803422 e-01
c	1.620226 e-02
α	2.126672e+00
P	1.031867 e+00
D	4.052195 e-03
q	4.052195 e-03
γ	0.36525 e+00

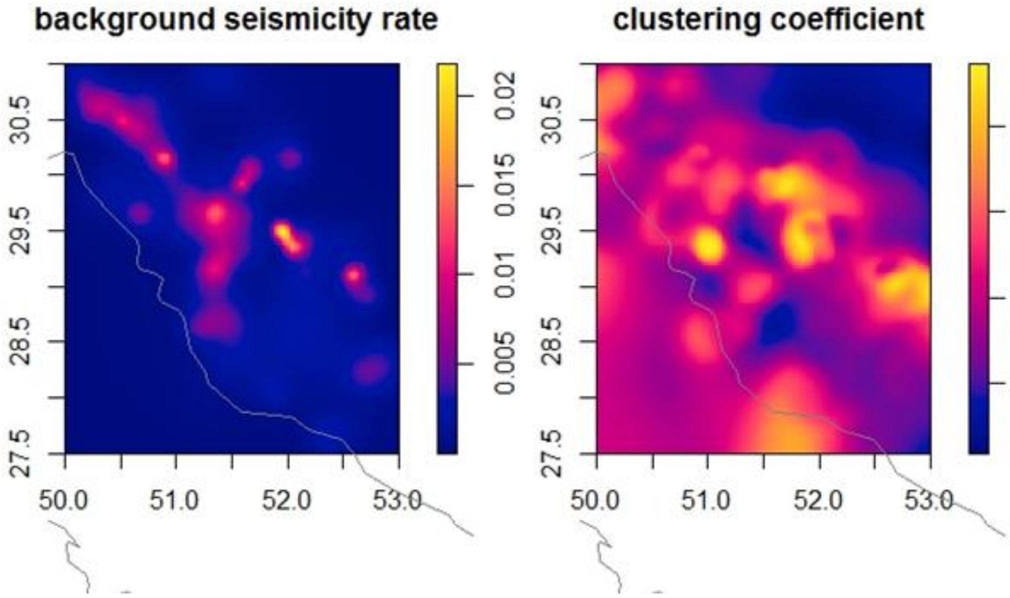

Figure 5. Plot of background seismicity rate and clustering coefficient for Study region

By subtracting estimated values of ETAS parameters into equations 5 and 6, we can calculate the probability of aftershocks for Kaki earthquake with magnitude Mw = 6.3. The forecasted number of aftershocks and the probability of aftershock occurrence, one day and one week after Kaki earthquake are presented in Tables 2 and 3 respectively. It is notable that, the expected number of aftershocks in table 2 are round up and are average value.

The quality and quantity of data is a key point in statistical analysis such as ETAS model. The magnitude versus time plot in figure 4 shows that only after 2004 the earthquakes with magnitude less than 5 were recorded in study area. Consequently, there are only 63 earthquakes in the catalog from 8/1/2004 to 4/7/2013. Therefore, it's difficult to select the exact date of starting point for analysis. The linear relation between Nt and t in figure 4 shows that the catalog used in the study has time-stationarity. But this catalog is incomplete due to nonlinear relationship in plot of log10(Nm) versus m (Gutenberg-Richter law) in figure 4.

Table 2. Forecasting aftershocks one day after 4/9/2013, Mw = 6.3 Bushehr earthquake.

Magnitude range of aftershocks	**Expected number of aftershocks**	**probability that at least one aftershock occur**	**Observed number of aftershocks in reality**
Mw = 4.0-5.0	12	99%	17
Mw = 5.0-5.5	0-1	40%	3
Mw > 5.5	0-1	10%	0

Table 3. Forecasting aftershocks one week after 4/9/2013, Mw = 6.3 Bushehr earthquake.

Magnitude range of aftershocks	**Expected number of aftershocks**	**probability that at least one aftershock occur**	**Observed number of aftershocks in reality**
Mw = 4.0-5.0	31	99%	39
Mw = 5.0-5.5	0-1	63%	3
Mw > 5.5	0-1	38%	0

5. CONCLUSIONS

In this article we use an epidemic type aftershock sequence (ETAS) model to investigate the space-time distribution of aftershocks in Bushehr province of Iran. Finally we try to forecast aftershocks within one week after Bushehr earthquake of Mw=6.3 in 2013. Our model underestimates the number of aftershocks to some extent. It my be (as Zhuang 2011says) due to increase in aftershock occurrence rate during the active triggering periods after mainshocks. This effect is not included in the equation 5. In recent years, aftershock forecasting knowledge has been developed in some countries such as United States, New Zealand and Japan. Aftershock forecasting experiments are still in early stages in the Iranian scientific community of seismology. It seems that more parametric studies are needed by using various catalogs and various models.

6. REFERENCES

Burkhard M, Grünthal G (2009). Seismic source zone characterization for the seismic hazard assessment project PEGASOS by the Expert Group 2 (EG1b). *Swiss Journal of Geosciences*, 102(1), 149-188.

Console R, Jackson DD, Kagan YY (2010). Using the ETAS model for catalog declustering and seismic background assessment. *Pure and Applied Geophysics*, Springer Basel Switzerland. 167(6-7), 819-830.

Gardner J K, Knopoff L (1974). Is the sequence of earthquakes in Southern California, with aftershocks removed, Poissonian?. *Bulletin of the Seismological Society of America*, 64(5), 1363-1367.

Helmstetter A, Kagan YY, Jackson DD (2006). Comparison of short term and time-independent earthquake forecast models for southern California, *Bulletin of the Seismological Society of America*, 96(1), 90–106.

Kanamori, H (1977). The energy release in great earthquakes. *Journal of geophysical research*, 82(20), 2981-2987.

Lombardi A M, Marzocchi W (2010). The ETAS model for daily forecasting of Italian seismicity in the CSEP experiment. *Annals of Geophysics*. Bologna, Italy.

Luen B (2010). Earthquake prediction: simple methods for complex phenomena. *Ph.D. Thesis*, Faculty of Statistics, University of California, Berkeley.

Ogata Y (1998). Space-time point-process models for earthquake occurrences. *Annals of the Institute of Statistical Mathematics*. The Institute of Statistical Mathematics, Tokyo Japan .50(2), 379-402.

Ogata Y (1999). Seismicity Analysis through Point-process Modelling: A Review. *Pure and Applied Geophysics*, Springer Basel Switzerland.155(2-4), 471-507.

Ogata Y (2006). Monitoring of anomaly in the aftershock sequence of the 2005 earthquake of M7. 0 o coast of the western Fukuoka, Japan, by the ETAS model. *Geophysical research letters*. 33(1).

Ogata Y (2011). Significant improvements of the space-time ETAS model for forecasting of accurate baseline seismicity. *Earth Planets and Space*. Springer japan.63(3), 217-229.

Omi T, Ogata Y, Hirata Y , Aihara K (2014). Estimating the ETAS model from an early aftershock sequence. *Geophysical Research Letters*, 41(3), 850-857.

Ommi S, Zafarani H, Zare M (2016). Aftershock decay rates in the Iranian plateau. *Pure and Applied Geophysics*, Springer Basel Switzerland. 173(7), 2305-2324.

Roeloffs E, Goltz J (2017). The California Earthquake Advisory Plan: A History. *Seismological Research Letters*, 88(3), 784-797.

Shahvar M P, Zare M, Castellaro S (2013). A unified seismic catalog for the Iranian plateau (1900–2011). *Seismological Research Letters*, 84(2), 233-249.

Stiphout T V, Zhuang J, Marsan D (2012). Seismicity declustering, Community Online Resource for Statistical Seismicity Analysis, doi:10.5078/corssa-52382934. Available at http://www.corssa.org.

Wells, D L, Coppersmith K J (1994). New empirical relationships among magnitude, rupture length, rupture width, rupture area, and surface displacement. *Bulletin of the seismological Society of America*, 84(4), 974-1002.

Yeo GL, CA Cornell (2005). Stochastic characterization and decision bases under time-dependent aftershock risk in performance-based earthquake engineering. *PEER Report 2005/13*. College of Engineering, Pacific Earthquake Engineering Research Center, University of California, Berkeley .

Zare M , Shahvar M (2013). Urgent Seismological Report on The 9 April 2013 Mw6.3 Kaki earthquake (Iran). http://www.iiees.ac.ir/fa/eqreports/.

Zare M, Amini H, Yazdi P, Sesetyan K, Demircioglu MB, Kalafat D, Erdik M, Giardini D, Asif Khan M, Tsereteli N (2014). Recent developments of the Middle East catalog. *Journal of seismology* . Springer 18(4), 749-772.

Zhuang J (2011). Next-day earthquake forecasts for the Japan region generated by the ETAS model. *Earth Planets and Space*. Springer japan, 63(3), 5.

Zhuang J (2012). Long-term earthquake forecasts based on the epidemic-type aftershock sequence (ETAS) model for short-term clustering. *Research in Geophysics*, 2(1), 8.

Zhuang J, Ogata Y, Vere-Jones D (2002). Stochastic declustering of space-time earthquake occurrences. *Journal of the American Statistical Association*, 97(458), 369-380.